X-625-76-220

PREPRINT

THE PLASMAPAUSE REVISITED

NELSON C. MAYNARD
JOSEPH M. GREBOWSKY

SEPTEMBER 1976

GSFC

GODDARD SPACE FLIGHT CENTER
GREENBELT, MARYLAND

The Plasmapause Revisited

Nelson C. Maynard
Joseph M. Grebowsky

Laboratory for Planetary Atmospheres
Goddard Space Flight Center
Greenbelt, Maryland 20771

September 1976

Abstract

Saturation of the DC double probe instrument on Explorer 45 has been used to identify the plasmapause. Fifteen months of this data resulted in a data base of sufficient size to statistically study the average position of the plasmapause over 14.5 hours of magnetic local time under differing magnetic conditions. The afternoon-evening bulge in the L coordinate of the plasmapause versus local time was found centered between 20 and 21 hours MLT during magnetically quiet periods and shifted toward dusk as activity increased, but always post dusk. During quiet periods a bulge in the L coordinate near noon was also seen, which disappeared as activity increased. The average local time distribution plasmapause position during high magnetic activity was irregular in the afternoon region where large scale convection models predict the creation of plasma-tails or detached plasma regions from increases in the solar wind induced convection.

The results suggest that solar wind induced convection is partially shielded from the dayside. As the intensity of the convection is increased, it more effectively penetrates the dayside, which shifts the post dusk bulge nearer to dusk and eliminates the quiet-time bulge near noon (created by Sq dynamo ionospheric electric fields projecting into the magnetosphere when dayside convection is weak). Correlations of the plasmapause L coordinate with Dst were more ordered than corresponding correlations with Kp with the maximum Kp over the previous 12 hours.

1. Introduction

Much has been written about the plasmapause: both experimental and theoretical covering the overall L - LT configuration of the plasmapause and more recently the dynamics of the plasmapause (see reviews by Chappell, 1972; Carpenter and Park, 1973; Rycroft, 1975). Most of the experimental evidence on the equatorial plasmapause configuration has come from two data sets, one derived from whistler determined equatorial densities (Carpenter, 1966) and the other from light ion density measurements by the Lockheed ion mass spectrometer on OGO-5 (see Chappell, 1971) (see the review by Rycroft, 1975, for a more complete list of earlier in situ measurements)

Many of the features of the whistler and OGO-5 deduced pictures of the plasmapause are similar, but definite differences exist. The most prominent difference is the average shape and position of the bulge in the plasmapause position in the afternoon-evening region. While Carpenter observed that the whistler detected bulge tends to be located after dusk, Chappell showed that the OGO-5 observations are consistent with a bulge centered at dusk. A bulge symmetrical about dusk is prevalent in many plasmaspheric models dating from that of Kavanagh et al. (1968) in which the solar wind induced convection is approximated by a constant dawn-to-dusk equatorial electric field.

The average plasmapause patterns have been limited in a statistical sense by the size of the data set in each case. It has been hard to sort out the behavior under varying conditions of magnetic activity due to the limited sampling available.

The Explorer 45 orbit with an apogee of 5.24 R_e geocentric, inclination of 3.6° and a period of 7 hours 49 minutes (Longanecker and Hoffman, 1973) is ideal for plasmapause studies in that the measurements are in the equatorial region and are of sufficient frequency to build a good statistical base.

While Explorer 45 carried no plasma density measuring instrument, the DC electric field instrument has been used to identify the plasmapause (Maynard and Cauffman, 1973; Cauffman and Maynard, 1974; Morgan and Maynard, 1976). At low plasma densities the instrument responds to spacecraft sheath potentials which are dependent upon both the ambient density and temperature. The crossing of the plasmapause is associated with the saturation of the instrument by these sheath potentials. The model of Cauffman and Maynard (1974) showed qualitatively that the saturation point is primarily a function of density. Morgan and Maynard (1976), using coincident ground based whistler and Explorer 45 DC probe observations, have set the most probable density of saturation at 60 electrons/cm^3 ± a factor of 2. Within the limits of defining the plasmapause location by a fixed plasma density (discussed in Section 3) the saturation of the electric field detector is a good indicator of a plasmapause traversal.

The Explorer 45 DC probe data has been previously used to trace the behavior of the plasmapause during magnetic storms in restricted local time regions (Maynard and Cauffman, 1973; Hoffman et al., 1975), to follow the development of isolated plasma regions (Maynard and Chen, 1975), and to provide information on the plasmapause in support of numerous other studies. In this paper we wish to investigate statistically the plasmapause behavior observed from Explorer 45 during various levels of magnetic activity.

2. Data Handling

The useable Explorer 45 data base for plasmapause measurements extended from launch in November, 1971, through February, 1973. After that period a malfunction in the data system prevented the gathering of analog data. During the useable period of 16 months, apogee moved from near 22 hours local time backward in time to near 10 hours local time, which allowed a coverage of over 12 hours of local time (this coverage is shown by the shaded area in Figure 1).

For each orbit the data were scanned to pick the times when the detector went into or came out of saturation. Points were selected only for which the detector remained in the new state (saturated or unsaturated) for a minimum of 1 minute. Each point was coded in three ways. An explanation of the first two codes is given in Table 1. The definition code (C1) is used to indicate whether or not saturation occurred and to specify if the saturation points correspond to the innermost transitions or to outer transitions (when multiple saturation regions were detected) on a given orbit. The steepness code (C2) was chosen rather arbitrarily from:(1) the consideration of the model calculations (Cauffman and Maynard, 1974), which indicated that transitioning the last 40% of the range to saturation most likely involved only a moderate density change, and (2) the scanning of early orbits, which indicated that distinction needed to be made between saturation events that occurred quickly and those that were spread out in time and space. The steepness code was based on universal time to facilitate data handling. Therefore the spatial extent of the transition to saturation will vary with L along the orbit for a fixed C2. Table 2 presents the change in L (ΔL) and the change in distance

traversed along the orbit (ΔD) at L values of 3, 4, and 5 for each of the 5 steepness codes which indicate saturation occurred. A third code, which will not be used here, was assigned to indicate oscillatory behavior (micropulsations) or other unordinary appearances of the data. In the case of no saturation throughout the orbit the apogee point was included in the data set with the appropriate codes.

The scanning of the useable Explorer 45 DC probe measurements resulted in a set of 4278 selected points of which 1866 were "primary" saturation events, i.e., the innermost points with C1 values of either 8 (outbound) or 9 (inbound). In addition to the C1 = 8 or 9 points there were 169 orbits on which saturation did not occur (C1 = 0 or 1).

The primary saturation events were grouped into windows of 1/2 hour magnetic local time (MLT) and sorted according to the codes. As will be discussed in Section 4, sorting was also done on Kp and Dst. For each sorting the average L position of these events within each MLT window was calculated along with the standard deviation from the mean. The number of points in each 1/2 hour window will be indicated around the perimeter of each figure describing the data. The total number of points plotted in any sorting will vary from case to case as no window containing less than 3 points was plotted. Windows at local times greater than 23 hours and less than 8.5 hours MLT were arbitrarily cut off as lacking adequate coverage in L (see Figure 1).

3. Implications of a constant density level for a plasmapause definition

The plasmapause physically refers to a sharp drop or "knee" in ionization as distance from the earth increases. Carpenter's (1963) original results referred to an order of magnitude drop from 400 to 40

electrons/cm^3, whereas Angerami and Carpenter (1966) typically showed a drop from several hundred down to 10 or less electrons/cm^3 in a distance of less than 0.15 R_e. With the advent of satellite measurements of the plasmapause, constant density definitions, such as 100 or 10 electrons/cm^3, were used to specify the plasmapause location in order to facilite data handling (Chappell et al., 1970a). Later this group also used the sharp density gradient definition (Chappell et al., 1971) to define an average plasmapause based on 150 profiles over all local times. Such a change was needed since the dusk OGO-5 observations showed the frequent occurrence of gradual ambient plasma density decreases to values below 10 ions/cm^3 without an abrupt plasmapause transition.

A constant density definition for the equatorial plasmapause location can lead to either a sharp knee type transition or a more gradual decrease in density being called a plasmapause. Since the saturation of the DC probe on Explorer 45 is primarily a function of the thermal plasma density we are limited to the fixed density definition (approximately 60 electrons/cm^3). Radial profiles from the Lockheed ion mass spectrometer on OGO-5 which are shown in Figure 13 and the left two of Figure 14 in Chappell's (1972) paper would cause the Explorer 45 instrument to saturate before a "physical plasmapause" was actually reached.

To provide a basis of comparison with the OGO-5 data the OGO-5 Lockheed spectrometer H^+ data profiles (obtained from the National Space Science Data Center) were scanned to pick the L value at which the level 60 ions/cm^3 was crossed. A plot of these is shown in Figure 2 with the number of points in each 1 hour window indicated around the edge. Basically, in the region where we have Explorer 45 data, the profile is

nearly circular between L = 4.5 and L = 5 with very little change noted with increasing Kp. A large scatter is seen as indicated by the 1 σ error bars. These data demonstrate that the plasmasphere bulge detected by Chappell et al., (1971) using the same data set, but selecting the abrupt changes, is not evident when a fixed density is chosen for the plasmapause without regard to the density gradient (the circular pattern for a fixed density was also found in the topside ionosphere by Brace and Theis, 1974).

Referring back to the meaning of the Explorer 45 steepness character C2 as defined in Table 2, it was decided to separate the DC probe saturation data into "sharp" crossings (C2 = 1, 2 or 3) and "gradient" crossings (C2 = 4 or 5) in order to distinguish between abrupt plasmapause transitions and gradual density transitions. The selected gradient crossings (770 out of the total data set number of 1866) within the magnetic index Kp ranges of a: Kp $\leq$ 1+, b: 1+ < Kp $\leq$ 3+ and c: Kp > 3+ are plotted in Figure 3. The average L position of the gradient saturation point varies little with local time except for the high Kp range for which there exists very few data points. This behavior is quite different from that of the sharp crossings which will be presented in the next section and, by comparison to Figure 2, confirms that these gradient points on the average correspond to a gradual density level transition rather that to a steep plasmapause-like gradient.

Therefore only the "sharp" crossings will be treated as true plasmapause crossings and will be used as such in the next section. While some overlap between gradual and abrupt density transitions has to exist in this plasmapause criteria, the results to be presented here and the previously cited studies which used the DC probe saturation to indicate the plasmapause position testify to its general validity.

4. Results

Figure 4 presents the sharp C2 = 1, 2 or 3 cases sorted according to Kp in the same manner as the gradual crossings in Figure 3. For quiet conditions (Figure 4a) a definite bulge in the plasmapause radius is seen centered between 20 and 21 hrs MLT. A suggestion of a bulge also exists near 12 hours MLT. As magnetic activity increases, the small noontime bulge disappears (Figure 4b) and the post dusk bulge is shifted nearer to dusk, centered between 19 and 20 hrs MLT. Note that the dayside plasmapause tends to move to lower L with increasing Kp as expected. A further increase in activity to Kp values > 3+ (Figure 4c) continues the above trends. In addition, the average location of the plasmapause in the region between 13 and 16 hrs MLT becomes more irregular. This is the center of the region where gross convection models predict tail-like structures arising from plasmapause reconfigurations initiated by large scale increases in the intensity of the solar wind induced convection (see Chen and Grebowsky, 1974) and where Chappell (1974) using OGO-5 observations found the maximum occurrence of "detached" cold plasma regions.

Figure 5 presents the same data set separated into four ranges of the Dst index: > -10, -10 to -30, -30 to -50, and < -50 gamma. In the quiet case the average bulge in the noontime plasmasphere is more evident when sorted on Dst (Figure 5a) than on Kp (Figure 4a). Again this bulge disappears as activity, reflected in Dst, is increased. The evening bulge, as in the Kp sorting, has its center located near 20-21 hrs. MLT during quiet times and moves toward dust with increasing activity. Note also the clear inward movement of the plasmapause on the

morning side with increasing negative Dst and the irregular region around 1400 hours at the higher Dst levels.

In general, sorting the plasmapause locations in terms of Dst ordered the data better than sorting on Kp or even in terms of the maximum Kp in the previous "X" hours. The plasmapause L versus Kp and versus Dst were plotted for each half hour MLT window. Using the maximum Kp in the previous X hours and continually increasing the interval X would reduce the scatter but only artificially, since as $X \rightarrow \infty$ the L vs max Kp plot tends to a vertical straight line. Hence X must be restricted to reasonably short times in order to retain significance. Figure 6 shows sample plots of L versus the maximum Kp over the past 12 hours (such a relationship was used to statistically order the nighttime plasmapause by Carpenter and Park, 1973). The same format is used in Figure 7 to show the dependence of the Explorer 45 plasmapause crossings on Dst. As can be seen the late morning and near midnight data orders well with Dst, much better than the corresponding Kp relationship seen in Figure 6. A small semblence of order is seen in the 16.5 to 17.0 hour plot in Figure 7 (and in adjacent time windows), but the plots from the post dusk bulge region and the afternoon plasmatail region show no obvious correlation between the plasmapause position and Dst. Since the plasmapause configuration is dependent on the time history of magnetic activity (see Chappell et al., 1970b) it was thought that averages of previous Kp's might better order the observations. However averaging Kp over intervals up to 15 hours did not order the data in this region either.

If the plasmasphere bulges in general after dusk and if a noontime bulge exists in quiet times, these facts should also reveal themselves

in the distribution of Explorer 45 orbits in which no plasmapause crossings were observed. The data set contained 169 such orbits. The number of such orbits whose apogee appears in each half hour MLT window is shown in the circular bar graph at the lower right of Figure 8. The remainder of Figure 8 depicts the sorting of these data with Dst. The basic pattern observed previously is also manifested here. The noontime bulge shifts into a post-noon plasmatail region, and the post-dusk bulge moves nearer dusk as activity increases, while the number of passes with no plasmapause crossings decreases as magnetic activity increases because of the inward motion of the plasmapause.

5. Discussion

Two currently accepted pictures of the near equatorial plasmapause have been derived from distinctly different data sets. Carpenter (1966) used whistler observations to derive an average profile for moderately disturbed periods (Kp = 2-4) which showed a plasmaspheric bulge commencing near dusk and centered between 19 and 20 hours. Chappell et al., (1971), using the sharp gradient transitions in the OGO-5 Lockheed ion mass spectrometer measurements of thermal H^+ densities (150 total points over all local time and all magnetic activity conditions), deduced an average plasmapause which was nearly symmetrical about dusk. Both profiles are shown in Figure 9. For comparison with these previous observations, the average Explorer 45 plasmapause position for $1+ < Kp \leq 3+$ (derived from 476 points distributed over 15 hours local time) has also been plotted in Figure 9. It is evident that the average post-dusk bulge observed by Explorer 45 compares more favorably with the whistler observations than the OGO-5 data. Further limiting the sharpness criteria of the DC probe saturation events,

to C2 = 1 or 2 only, produced even better agreement with Carpenter's result although the more limited statistics resulted in an increase in the standard deviation in some areas.

The larger extent of the bulge deduced from the OGO-5 measurements is partially the result of the greater sensitivity of that instrument compared to the other techniques (recording steep gradients at 10 electrons/cm^3 and below), the covering of all magnetic activity levels and the fact that the Explorer 45 orbit and the whistler observations did not extend out to the larger L values. The reason for the approximate symmetry about dusk of the OGO-5 detected bulge in contrast to the post-dusk bulges observed in the other two data sets is not clear; however, it partially may be related to the more limited statistics of the OGO observations. Even the addition of actual plasmapause locations at the times of those Explorer 45 orbits that did not encounter a plasmapause would not make the currently deduced plasmapause topology symmetrical about dusk since the distribution of such passes was peaked in the regions of the noon and post-dusk bulges (Figure 7). The existence of sharp density gradients further out than Explorer 45's orbit at the time of the observed C2 = 4 and 5 saturation cases, which were omitted from the data set, might possibly account for some of the differences between the observations, as these were more symmetrically distributed in local time. However, the conclusion can be drawn that the whistler and Explorer 45 post-dusk plasmaspheric bulge represents the average behavior of steep plasma density gradients in the equatorial plane transitioning through 60 electrons/cm^3.

What are the implications of a post-dusk bulge? Models of the plasmapause configuration are often derived on the basis of an equatorial

convection electric field, which is assumed to penetrate throughout the magnetosphere, interacting with the electric field representing the co-rotational motion of plasma tied by magnetic field lines with the earth. A uniform equatorial convection field directed from dawn to dusk combined with co-rotation results in a neutral point at dusk and a "tear-drop" electric equipotential line from that point which under steady state conditions depicts the plasmapause (see Figure 10a). Such a field results in a bulge symmetric about dusk. If the convection electric field was completely shielded from the dayside of the earth (possibly due to the high conductivity in the dayside ionosphere), the equipotentials corresponding to the solar wind induced convection might appear as in Figure 10b. When this convection pattern is combined with co-rotation the flow neutral point is shifted to 21 hrs and corresponds to the apex of the associated "tear-drop" plasmaspheric configuration under steady state conditions (see Figure 10c) (Grebowsky, 1971). Indeed, Wolf (1970) derived steady state patterns assuming various ionospheric conductivities by solving $\nabla \cdot \vec{J} = 0$ for various magnetospheric potentials and showed how the higher dayside conductivities could short out the convection field and how such an effect tends to produce post-dusk asymmetries in the equipotentials. Rycroft (1974) further showed how the steady state plasmasphere bulge moves toward dusk from 21 hours LT as the solar wind induced convection is allowed to penetrate more and more into the dayside of the earth. It should be noted that it is still not known which models represent best the actual ambient convection electric field.

Thus, from the existing convection models, a post-dusk plasmaspheric bulge implies that the solar wind induced convection electric field is at

least partially shielded from the dayside of the magnetosphere. Although Wolf (1970) has shown that a band of enhanced conductivity in the auroral zone, such as one might expect during storm conditions, could pull the bulge toward the nightside of dusk, the observed shift toward the nightside is greatest under quiet conditions. The fact that the bulge moves toward dusk with increasing magnetic activity would indicate that the dayside shielding becomes less effective for larger convection fields and accounts for the observations. However, it should be noted that a portion of the observed movement toward dusk could arise from temporal variations in which the bulge is moving in immediate response to an enhancement in convection as deduced by Carpenter (1970) and Nishida (1971).

A quiettime bulge near local noon (see Figure 4a) was suggested in Carpenter's (1966) original whistler derived density profile. A day-night asymmetry in the plasmasphere with the noon radius larger than the nighttime radius was also suggested by Prognoz measurements (Gringauz and Bezrukikh, 1975), although these measurements did not conclusively show a dayside bulge. Carpenter and Seeley (1976) have studied radial thermal plasma drift patterns during quiet periods by following the movement of whistler ducts. Their drift patterns, which they interpret as evidence of the Sq dynamo electric field system, show an outward drift in the morning hours followed by an inward drift in the afternoon hours. Such a pattern would clearly correspond to a noontime bulge in the average plasmapause configuration. Even though Morgan (1976) has shown that radial whistler duct motions can be used to infer electric fields only if the ambient plasma is co-rotating with the earth, this criteria should be satisfied during the quiet steady state periods selected for study by Carpenter and Seeley.

If the noontime bulge (Figure 5a) is created by dynamo fields, then the solar wind induced convection fields must be comparitively weak in the dayside of the magnetosphere at the time of such observations. This fits with the picture discussed earlier of partial shielding of the convection fields over the dayside. The disappearance of the noontime bulge with increasing magnetic activity also fits the previous picture in that the shielding is less effective when convection is increased (i.e., magnetic disturbances are increased). Further evidence for an increase in dayside convection with increases in magnetic activity is given in Maynard and Chen (1975) where the development of isolated plasma regions is discussed.

While definite order was seen in the correlation between the plasmapause L position with Dst near midnight and in the pre-noon hours, the observations in the bulge and plasmatail regions in general exhibited a large amount of scatter. Although no clear explanation of this scatter yet exists, a number of possibilities can be advanced. First and foremost is the fact that the indices Dst and Kp represent global averages of phenomena over periods of 1 hr and 3 hours respectively. Substorm effects on the other hand are more limited spatially and occur over shorter time scales. Also the plasmapause is dependent on past history as well. Multiple plasmapause-like boundaries may exist due to incomplete filling of flux tubes following magnetic storms (see Figure 14 of Chappell, 1972). The convection or co-rotation of localized plasmapause perturbations away from their point of origin is another factor.

Just as it is clear that order can not be obtained in all regions by comparing the observed plasmapause locations to large scale magnetic indices,

it is also clear that the large scale convection models depending on these indices will suffer the same fate. The models have been useful in describing many of the large scale features. Statistical relationships between the plasmapause location and L have been given by Binsack (1967), Carpenter (1967) and numerous authors since (see Kivelson, 1976). Due to the statistical uncertainties in such correlations, little would be gained by relating such functional forms to the current data set. For this reason no Dst or Kp vs L relationship will be given from this data.

The fact that Dst was better than Kp as an ordering factor implies a relationship between the ring current intensity and the plasmapause position. In considering this, it is possible that the plasmapause position should be the controlling factor since cold plasma interactions are a mechanism for ring current decay (e.g. Williams and Lyons, 1974). Or this may just reflect the fact that the distributions of the energetic ring current ions (related to D_{st}) and the thermal ions (associated with the plasmapause) both respond in step with changes in the convection electric field (e.g., Grebowsky and Chen, 1975).

Acknowledgement: We wish to acknowledge Dr. R. A. Hoffman for helpful comments on the manuscript.

Table 1: Explanation of Codes

Definition Code - C1

0	No saturation of detector - saturation was not approached (< 60% full scale)
1	No saturation of detector - signal approached saturation (> 60% full scale)
6	Intermediate transition: unsaturated to saturated
7	Intermediate transition: saturated to unsaturated
8	Initial transition: unsaturated to saturated (usually outbound)
9	Final transition: saturated to unsaturated (usually inbound)

Steepness Code - C2

0	No saturation
1	Transition from 60% of full scale to saturation occurs in less than 30s.
2	Above transition occurs in between 30s and 3 minutes
3	Above transition occurs in between 3 and 10 minutes
4	Above transition occurs in between 10 and 30 minutes
5	Above transition occurs in greater than 30 minutes

Table 2: Steepness Factor

	ΔL(L) at L of			ΔD(km)(along orbital track) at L of		
	3	4	5	3	4	5
1	0.0 - 0.02	0 - 0.01	0 - 0.006	0 - 150	0 - 110	0 - 78
2	0.02 - 0.10	0.01 - 0.07	0.006 - 0.04	150 - 900	110 - 670	78 - 470
3	0.10 - 0.33	0.07 - 0.23	0.04 - 0.12	900 - 3000	670 - 1100	470 - 1600
4	0.33 - 1.00	0.23 - 0.69	0.12 - 0.36	3000 - 9000	1100 - 6700	1600 - 4700
5	> 1.00	> 0.69	> 0.36	> 9000	> 670C	> 4700

References

Angerami, J. J., and D. L. Carpenter, Whistler studies of the plasmapause in the magnetosphere, 2, electron density and total tube electron content near the knee in magnetospheric ionization, J. Geophys. Res., 71, 711, 1966.

Binsack, J. H., Plasmapause observations with the M.I.T. experiment on Imp 2, J. Geophys. Res., 72, 5231, 1967.

Brace, L. H., and R. F. Theis, The behavior of the plasmapause at mid-latitudes: ISIS-I Langmuir probe measurements, J. Geophys. Res., 79, 1871, 1974.

Carpenter, D. L., Whistler evidence of a 'knee' in the magnetospheric ionization density profile, J. Geophys. Res., 68, 1675, 1963.

Carpenter, D. L., Whistler studies of the plasmapause in the magnetosphere, 1, temporal variations in the position of the knee and some evidence of plasma motions near the knee, J. Geophys. Res., 71, 693, 1966.

Carpenter, D. L., Relations between the dawn minimum in the equatorial radius of the plasmapause and Dst, Kp and local K at Byrd Station, J. Geophys. Res., 72, 2969, 1967.

Carpenter, D. L., Whistler evidence of the dynamic behavior of the dusk side bulge in the plasmasphere, J. Geophys. Res., 3837, 1970.

Carpenter, D. L., and C. G. Park, On what the ionospheric worker should know about the plasmapause-plasmasphere, Rev, Geophys. Space Phys, 11, 133, 1973.

Carpenter, D. L., and N. T. Seely, Cross-L plasma drifts in the outer plasmasphere: quiet time patterns and some substorm effects, J. Geophys. Res., 81, 2728, 1976.

Caufmann, D. P., and N. C. Maynard, A model of the effect of the satellite photosheath on a double floating probe system, J. Geophys. Res., 79, 2427, 1974.

Chappell, C. R., Recent satellite measurements of the morphology and dynamics of the plasmasphere, Rev. Geophys. Space Phys., 10, 951, 1972.

Chappell, C. R., Detached plasma regions in the magnetosphere, J. Geophys. Res., 79, 1861, 1974.

Chappell, C. R., K. K. Harris, and G. W. Sharp, A study of the influence of magnetic activity on the location of the plasmapause as measured by OGO 5, J. Geophys. Res., 75, 50, 1970a.

Chappell, C. R., K. K. Harris, and G. W. Sharp, The monphology of the bulge region of the plasmasphere, J. Geophys. Res., 75, 3848, 1970b.

Chappell, C. R., K. K. Harris, and G. W. Sharp, The dayside of the plasmasphere, J. Geophys. Res., 76, 7632, 1971.

Chen, A. J., and J. M. Grebowsky, Plasma tail interpretations of pronounced detached plasma regions measured by OGO-5, J. Geophys. Res., 79, 3851, 1974.

Grebowsky, J. M., Time-dependent plasmapause motion, J. Geophys. Res., 76, 6193, 1971.

Grebowsky, J. M., and A. J. Chen, Effects of convection electric field on the distribution of ring current type protons, Planet Space Sci., 23, 1045, 1975.

Gringauz, K. I., and V. V. Bezrukikh, Asymmetry of Earth's plasmasphere in direction noon-midnight from data of measurements on satellites Prognoz and Prognoz 2, report D-217, Space Research Institute, Academy of Sciences, USSR, Moscow, 1975.

Hoffman, R. A., L. J. Cahill, Jr., R. R. Anderson, N. C. Maynard, P. H. Smith, T. A. Fritz, D. J. Williams, A. Konradi, and D. A. Gurnett, Explorer 45 (S^3-A) observations of the magnetosphere and magnetopause during the August 4-6, 1972, magnetic storm period, J. Geophys. Res., 80, 4287, 1975.

Kavanagh, L. D., Jr., J. W. Freeman, Jr., and A. J. Chen, Plasma flow in the magnetosphere, J. Geophys. Res., 73, 5511, 1968.

Kivelson, M. G., Magnetophspheric electric fields and their variation with geomagnetic activity. Rev. Geophys. and Space Phys., 14, 189, 1976.

Longanecker, G. W., and R. A. Hoffman, S^3-A spacecraft description, J. Geophys. Res., 78, 4711, 1973.

Maynard, N. C., and D. P. Cauffman, Double floating probe measurements on S^3-A, J. Geophys. Res., 78, 4745, 1973.

Maynard, N. C., and A. J. Chen, Isolated cold plasma regions: observations and their relation to possible production mechanisms, J. Geophys. Res., 80, 1009, 1975.

Morgan, M. G., Simultaneous observations of whistlers at two $L \simeq 4$ Alaskan stations, J. Geophys. Res., 81, 3977, 1976.

Morgan, M. G., and N. C. Maynard, Evidence of dayside plasmaspheric structure through comparisons of ground-based whistler data and Explorer 45 plasmapause data, J. Geophys. Res., 81, 3992, 1976.

Nishida, A., Deformation of the duskside plasmapause, Cosmic Electrodynamics, 2, 340, 1971.

Rycroft, M. J., A review of in situ observations of the plasmapause, Ann. Geophys., 31, 1, 1975.

Rycroft, M. J., Magnetospheric plasma flow and electric fields derived from whistler observations, in Correlated Interplanetary and Magnetospheric Observations, ed. by D. E. Page, D. Reidel Publ. Co., Dordrecht, p. 317, 1974.

Williams, D. J., and L. R. Lyons, Further aspects of the proton ring current interaction with the plasmapause: main and recovery phases, J. Geophys. Res., 79, 4791, 1974.

Wolf, R. A., Effects of ionospheric conductivity on convective flow of plasma in the magnetosphere, J. Geophys. Res., 75, 4677, 1970.

Figure Captions

Figure 1: The initial and final orbits of Explorer 45 used in the data set. The shaded area defines the region over which adequate coverage in L existed to be considered in the statistical plots.

Figure 2: Crossings of the level 60 ions/cm^3 as determined by the Lockheed ion mass spectrometer on OGO-5. The data is sorted into two ranges of Kp (< 3 and ≥ 3). The error bars show the standard deviation from the mean for each Kp range.

Figure 3: The average local time dependence of the "gradient" saturation events detected on Explorer 45 (C2 = 4 or 5; see text). The data is sorted into Kp intervals of (a) Kp $\leq$ 1+, (b) 1 + $<$ Kp $\leq$ 3+ and (c) Kp $>$ 3+. In this figure and also in Figures 4 and 5 the number of points within each half hour local time window is given around the periphery. The shaded area represents the standard deviation from the mean.

Figure 4: The average local time dependence of the sharp saturation events detected on Explorer 45 (C2 = 1, 2 or 3; see text) and interpreted as plasmapause crossings. The data is sorted into Kp intervals of (a) Kp $\leq$ 1+, (b) 1+ $<$ Kp $\leq$ 3+, and (c) Kp $>$ 3+. (See also Figure 3 caption.)

Figure 5: The average local time dependence of the same data selection as Figure 4 but sorted according to the Dst index. The ranges of Dst are (a) Dst $>$ -10, (b) -10 $>$ Dst $>$ =30, (c) -30 $>$ Dst $>$ -50, and (d) Dst $<$ -50. (See also Figure 3 caption).

Figure 6: Sample plots of the behavior of the plasmapause L position versus the maximum Kp over the previous 12 hours. The magnetic local time window covered is given in each plot.

Figure 7: The same data as in Figure 6 plotted versus the Dst index.

Figure 8: Bar graphs of the total number of orbits whose apogee falls in each half-hour window and on which there was no saturation of the DC probe data, i.e., no plasmapause crossing. The data is sorted according to the Dst index: (a) $-30 > Dst > -50$, (b) $-10 > Dst > -30$, (c) $Dst > -10$, and (d) all cases.

Figure 9: The average plasmapause L versus local time profile as determined from whistler observations (Carpenter, 1966), the OGO-5 ion mass spectrometer data (Chappell et al., 1971), and the Explorer 45 DC probe data (from Figure 4b)

Figure 10: (a) Equipotential contours resulting from superimposing a uniform convection field on the electric field representing co-rotation. The shaded area represents the steady state plasmasphere defined by this type of model. (b and c) A hypothetical convection pattern resulting from a field which is completely shielded from the dayside (b) and the resulting equipotential pattern (c) when that field is combined with co-rotation (from Grebowsky, 1971). Again the shaded area in (c) represents the plasmasphere defined by this convection pattern.

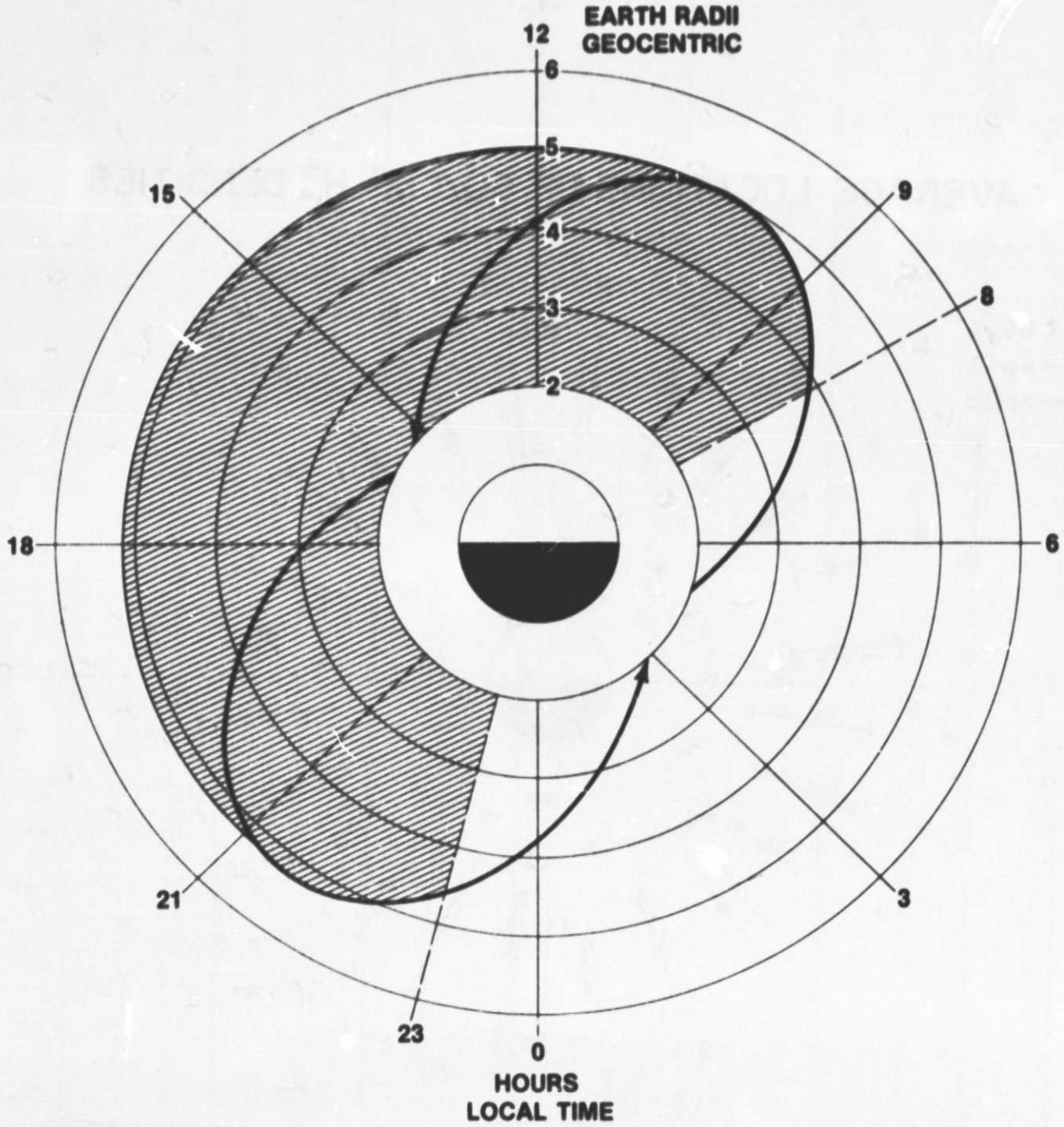
EARTH RADII
GEOCENTRIC
12
6
5
4
3
2
15
9
8
18
6
21
3
23
0
HOURS
LOCAL TIME

Figure 1

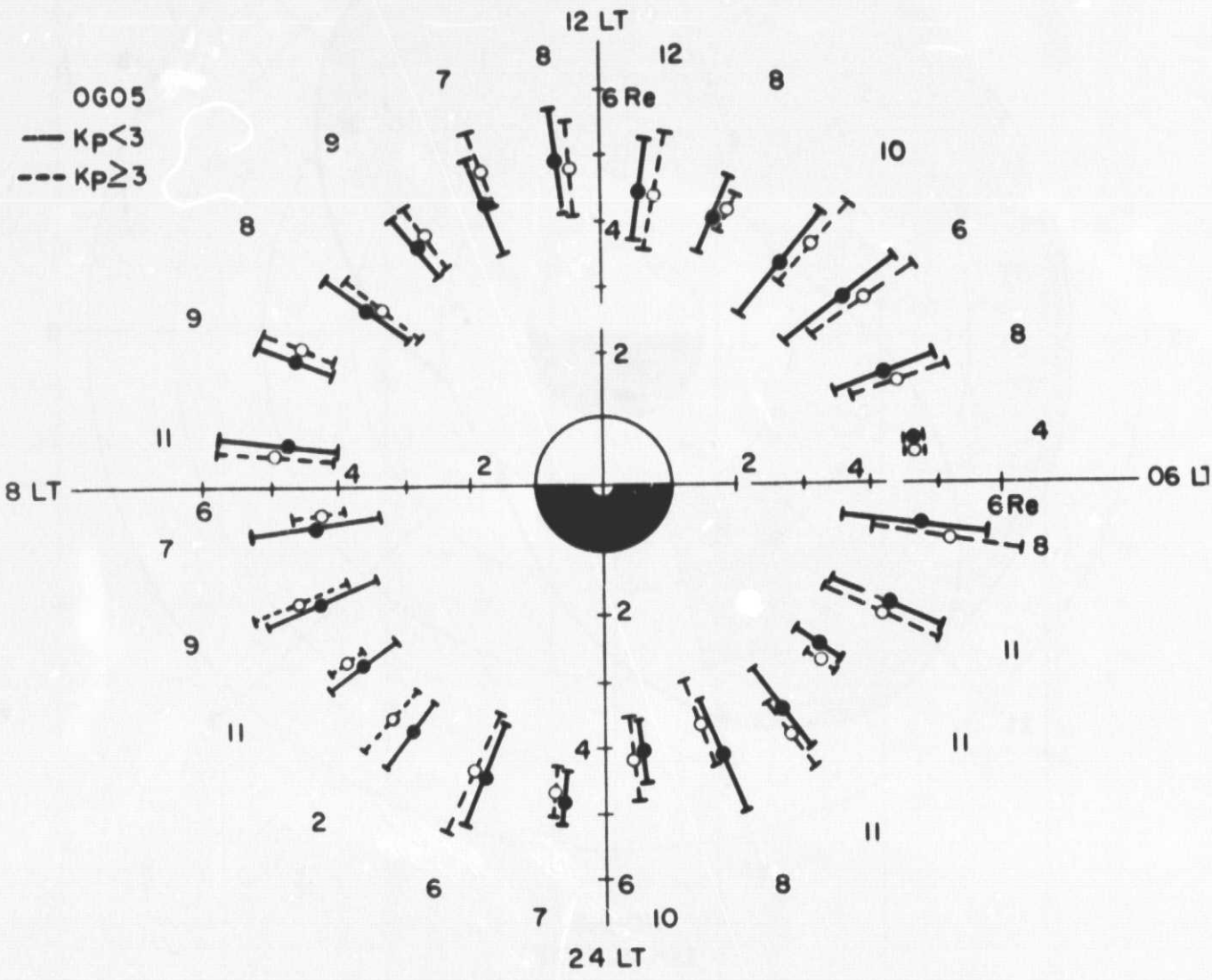
AVERAGE LOCATIONS OF 60/Cm3 H+ DENSITIES
12 LT
24 LT
8 LT
06 LT
6 Re
6 Re
OGO5
Kp<3
Kp≥3

Figure 2

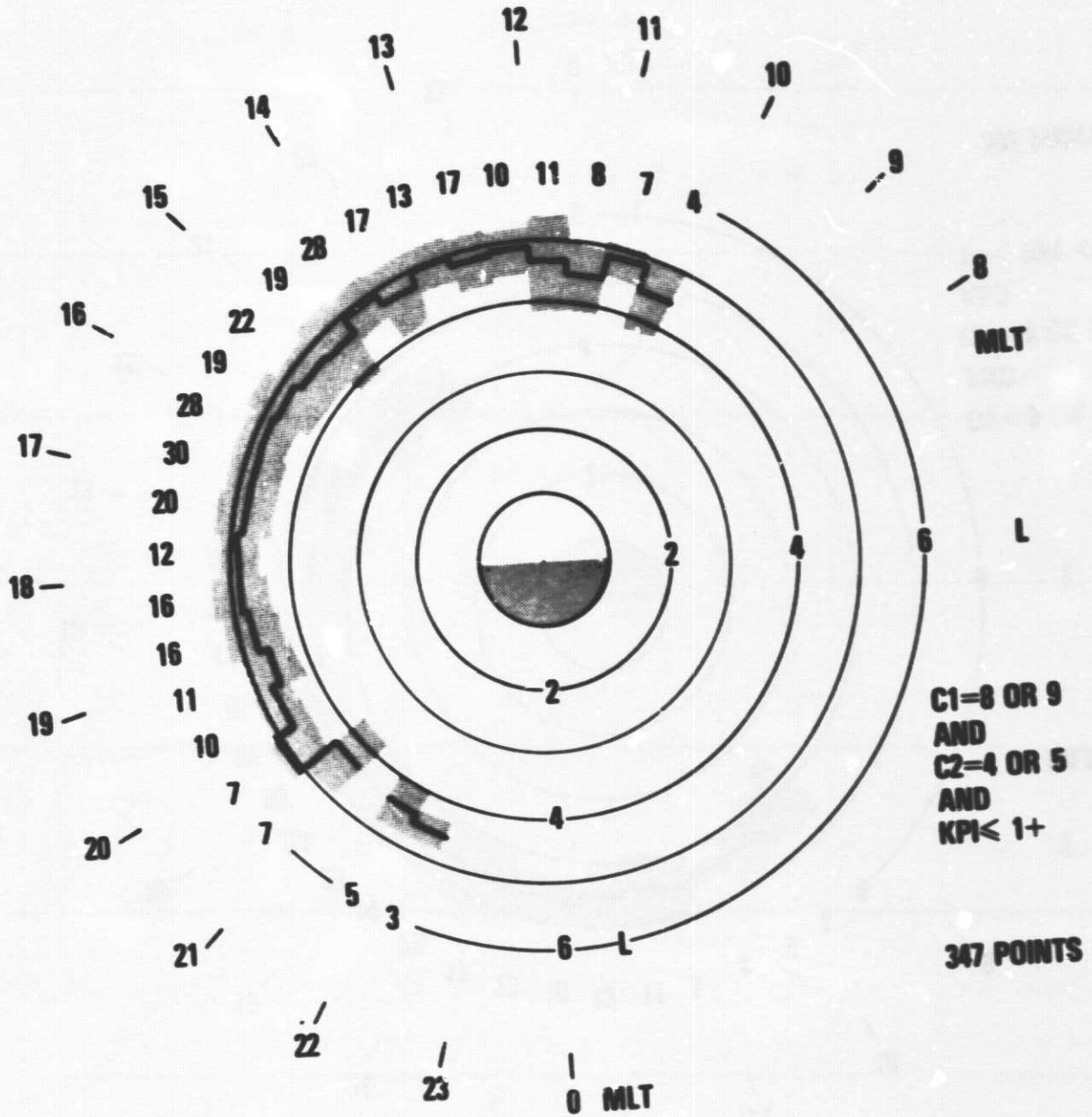
12
11
13
10
14
9
15
8
MLT
16
17
18
19
20
21
22
23
0 MLT
L
2
4
6
C1=8 OR 9
AND
C2=4 OR 5
AND
KPI≤ 1+
347 POINTS

Figure 3a

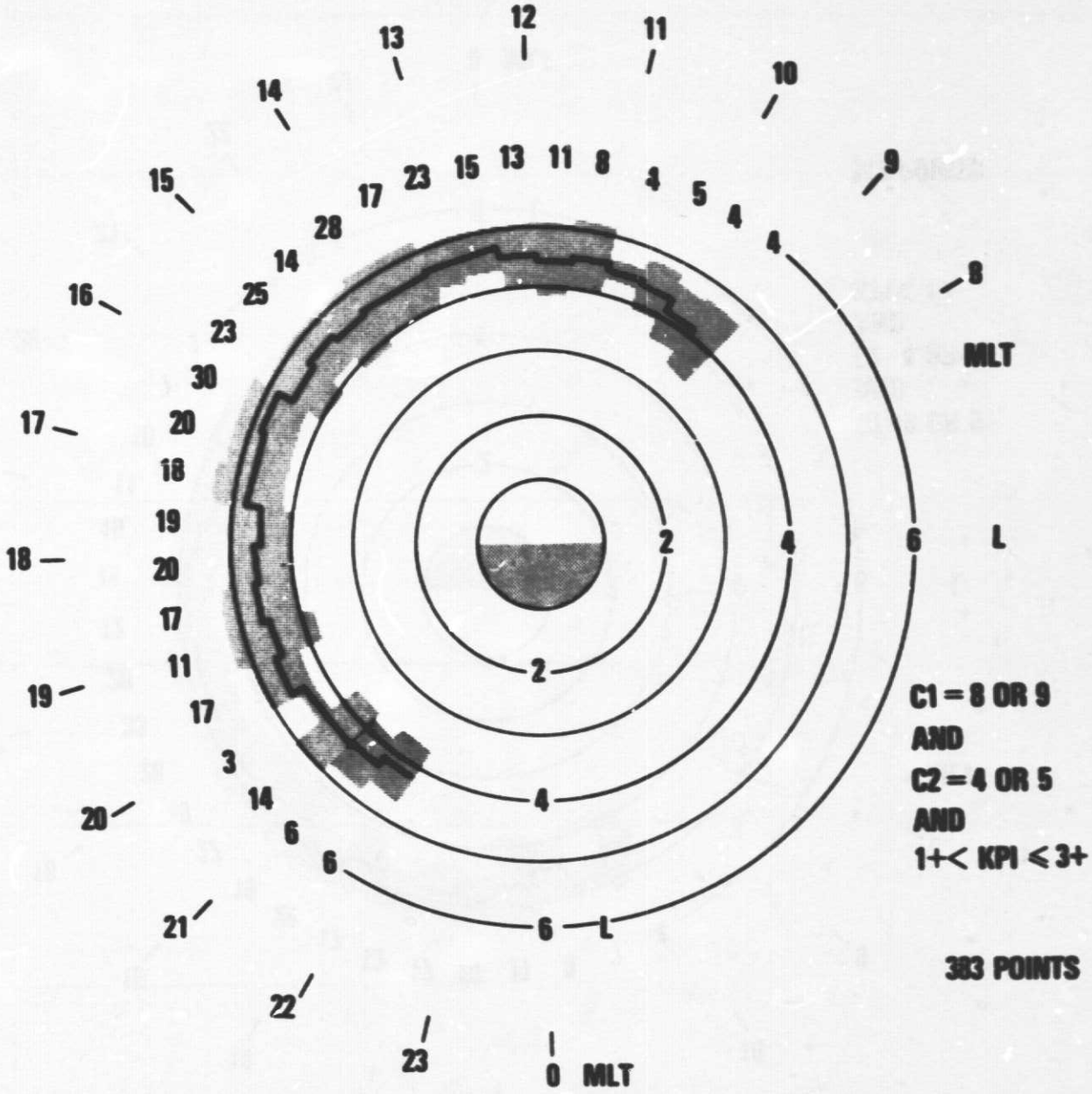
12
13
11
14
10
15
9
16
8
MLT
17
18
19
L
20
21
22
23
0 MLT
C1 = 8 OR 9
AND
C2 = 4 OR 5
AND
1+< KPI ≤ 3+
383 POINTS

Figure 3b

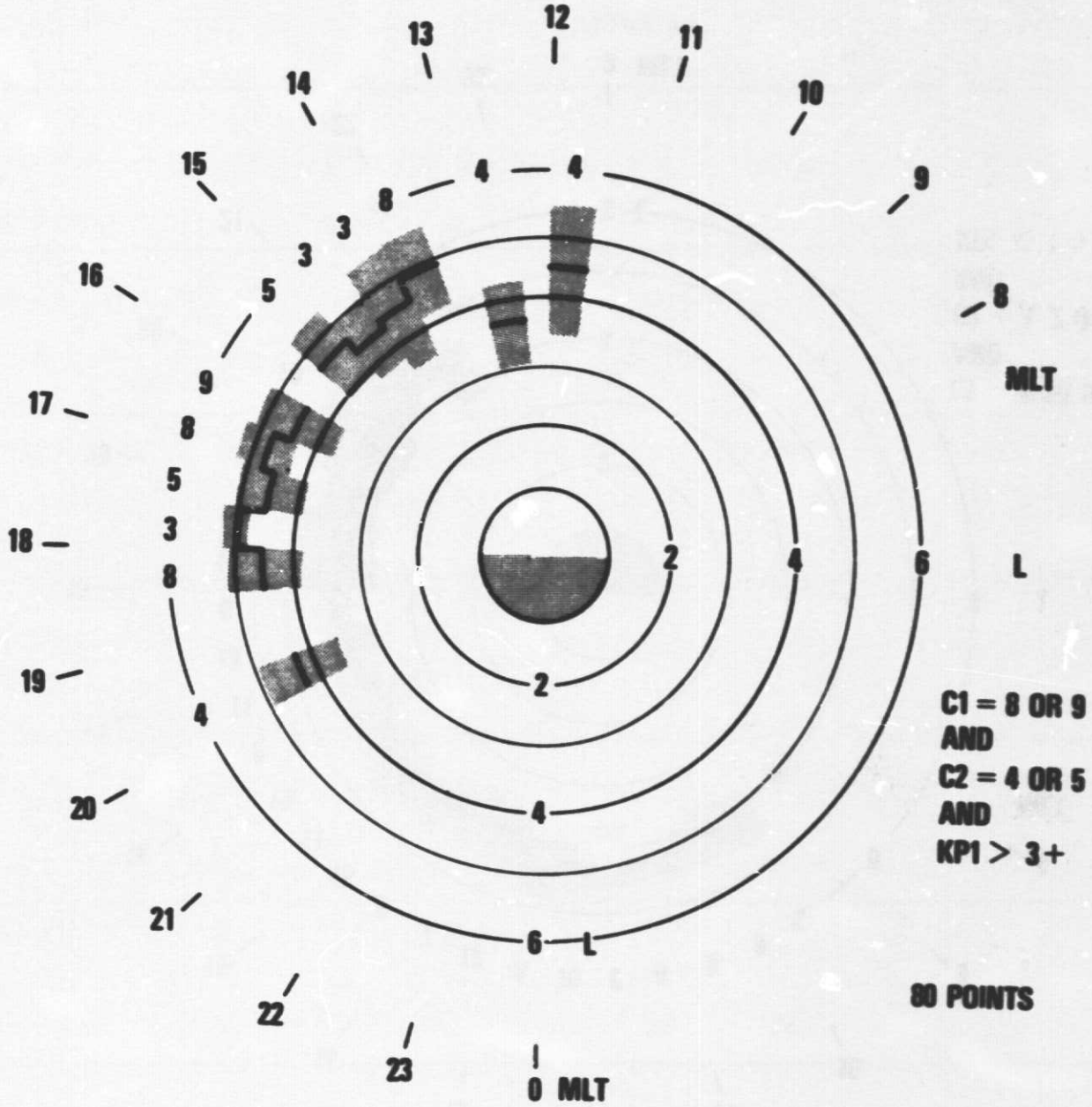
12
13
11
14
10
15
9
16
8
17
MLT
18
L
19
20
21
22
23
0 MLT
C1 = 8 OR 9
AND
C2 = 4 OR 5
AND
KP1 > 3+
80 POINTS

Figure 3c

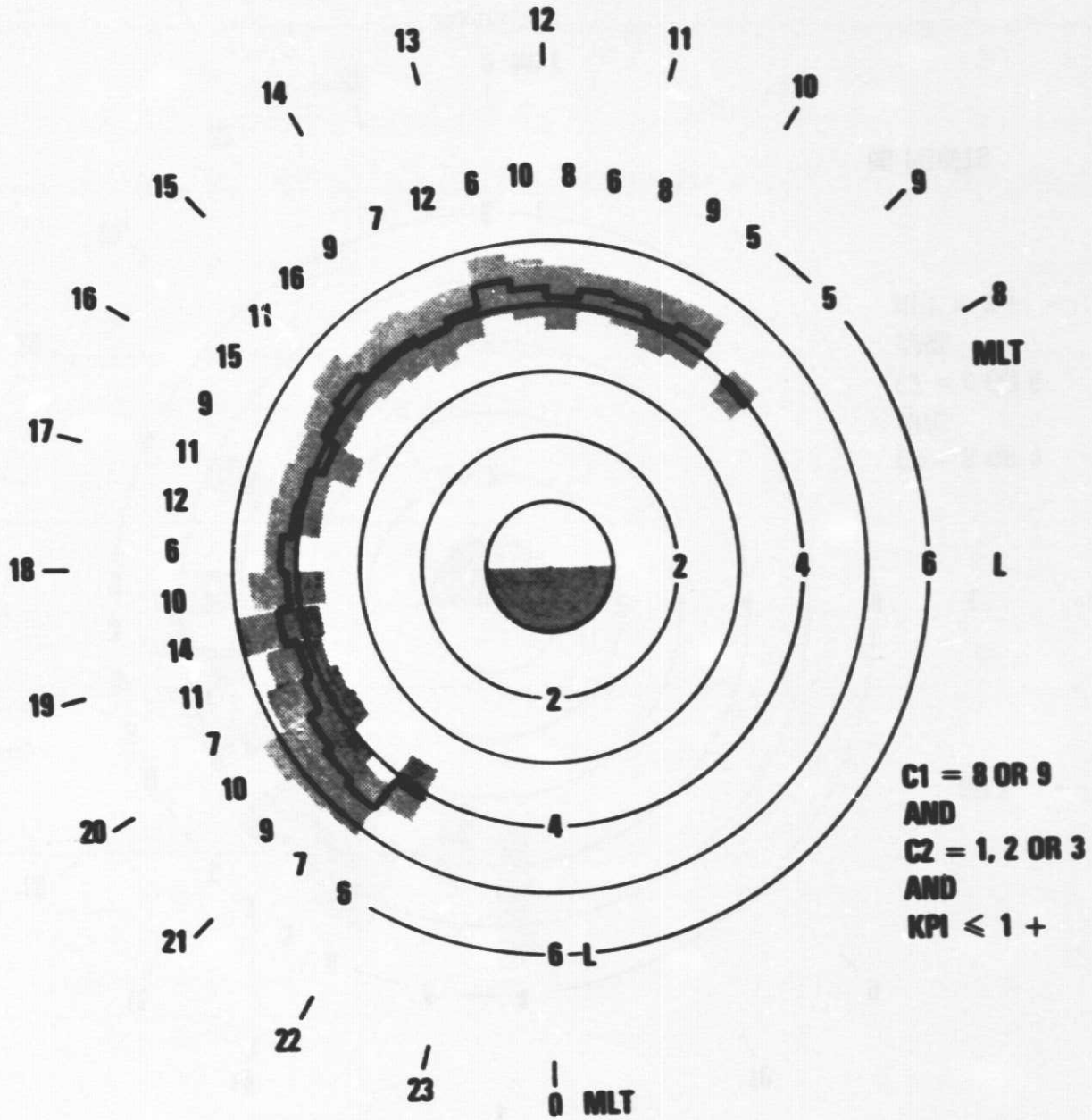
12
13
11
14
10
15
9
16
8
MLT
17
18
19
20
21
22
23
0 MLT
L
2
4
6
C1 = 8 OR 9
AND
C2 = 1, 2 OR 3
AND
KP1 ≤ 1 +

Figure 4a

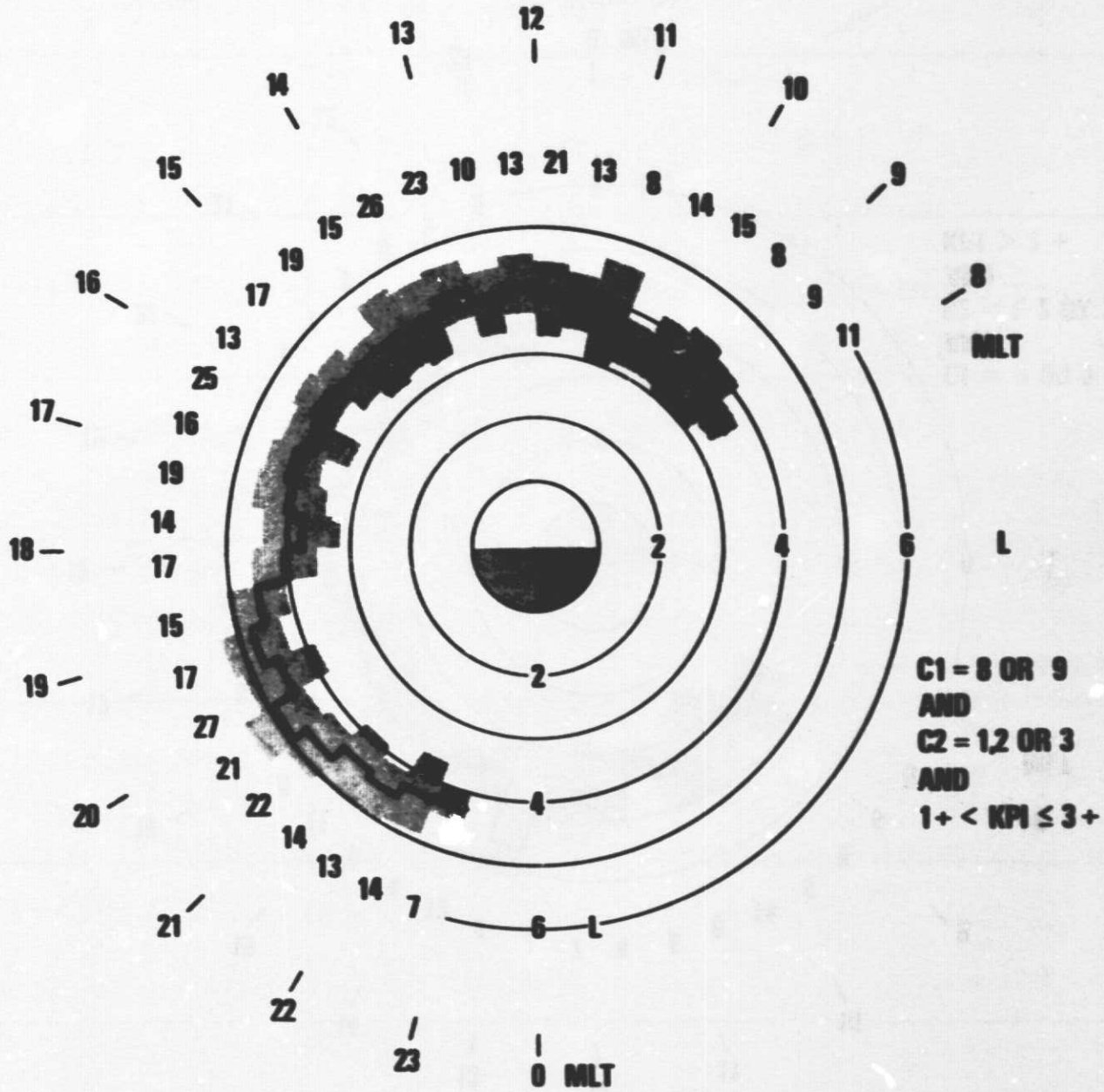

Figure 4b

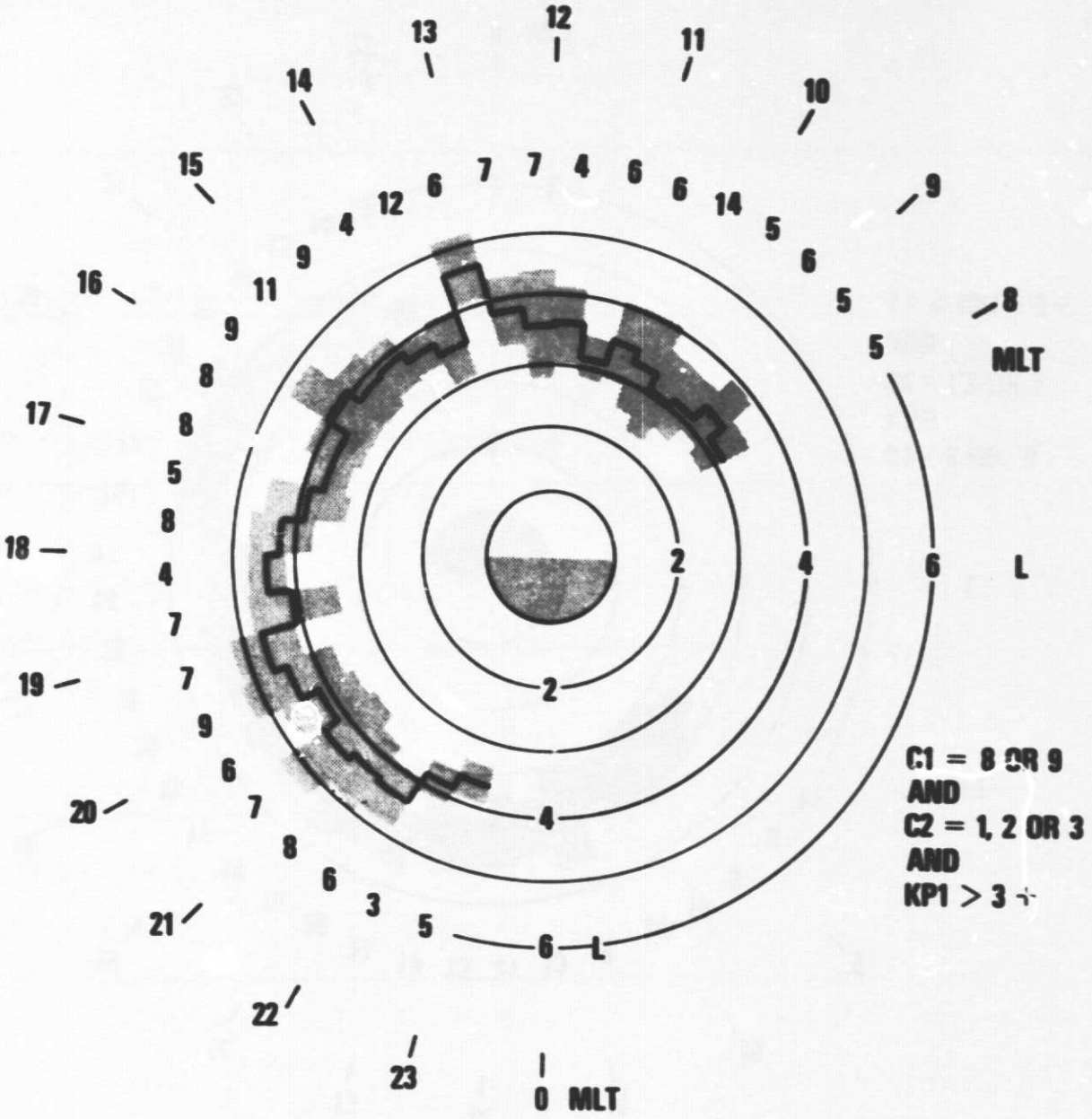
12
13
11
14
10
15
9
16
8
MLT
17
18
L
19
20
21
22
23
0 MLT
2
4
6
C1 = 8 OR 9
AND
C2 = 1, 2 OR 3
AND
KP1 > 3+

Figure 4c

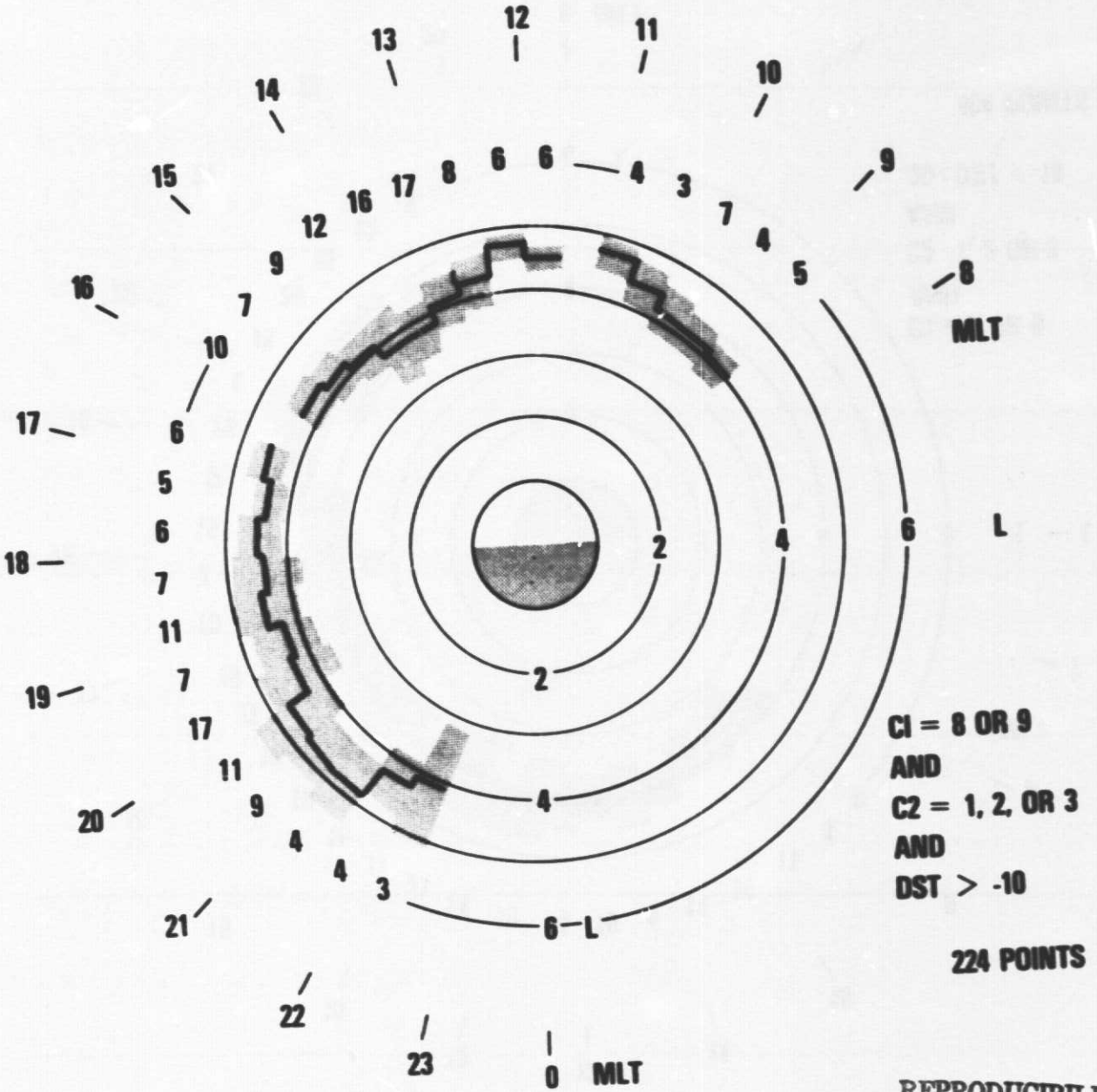

Figure 5a

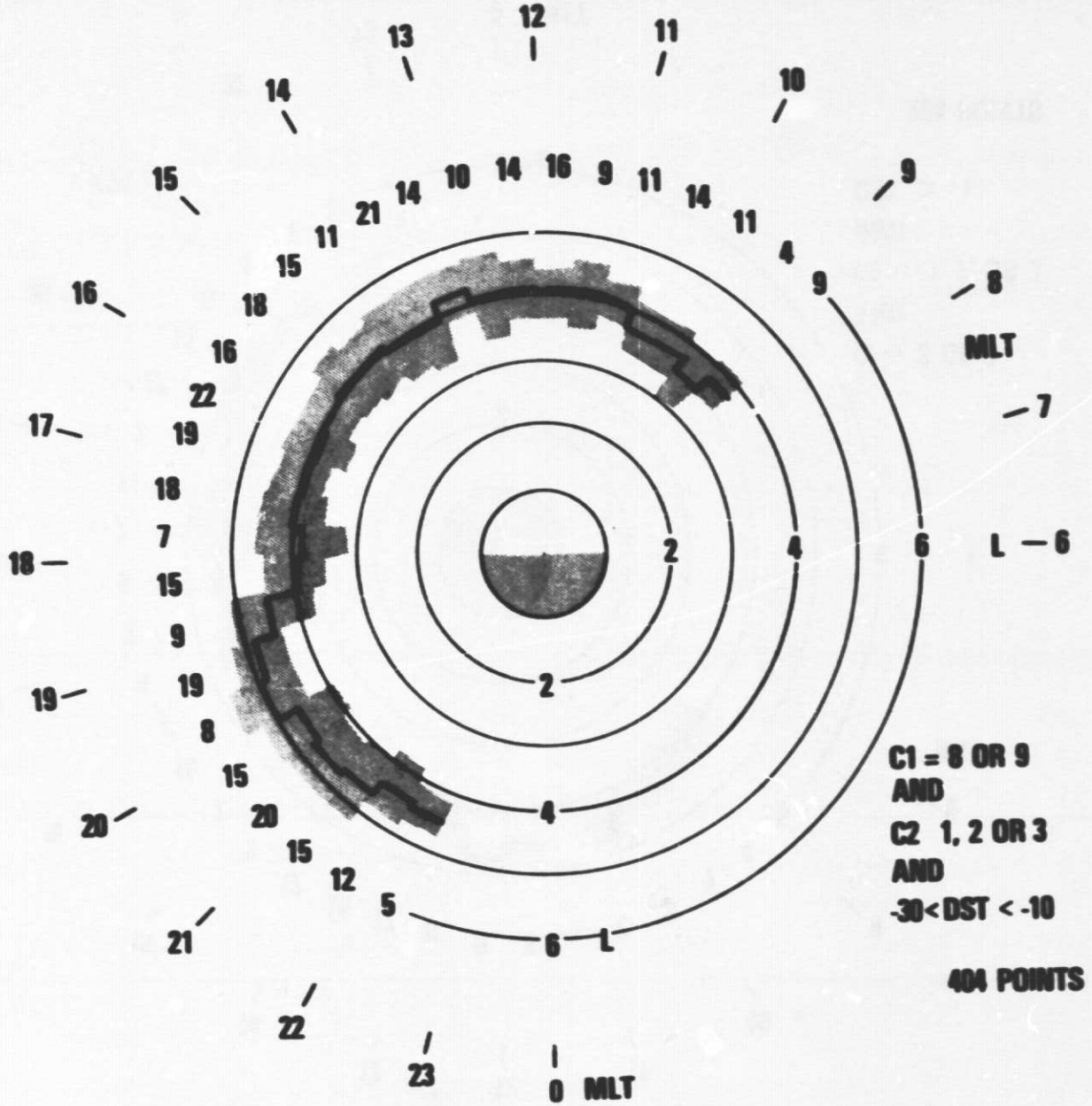
12
13
11
14
10
15
9
16
8
MLT
17
7
18
L — 6
19
20
21
22
23
0 MLT
2
4
6
L
C1 = 8 OR 9
AND
C2 1, 2 OR 3
AND
-30< DST < -10
404 POINTS

Figure 5b

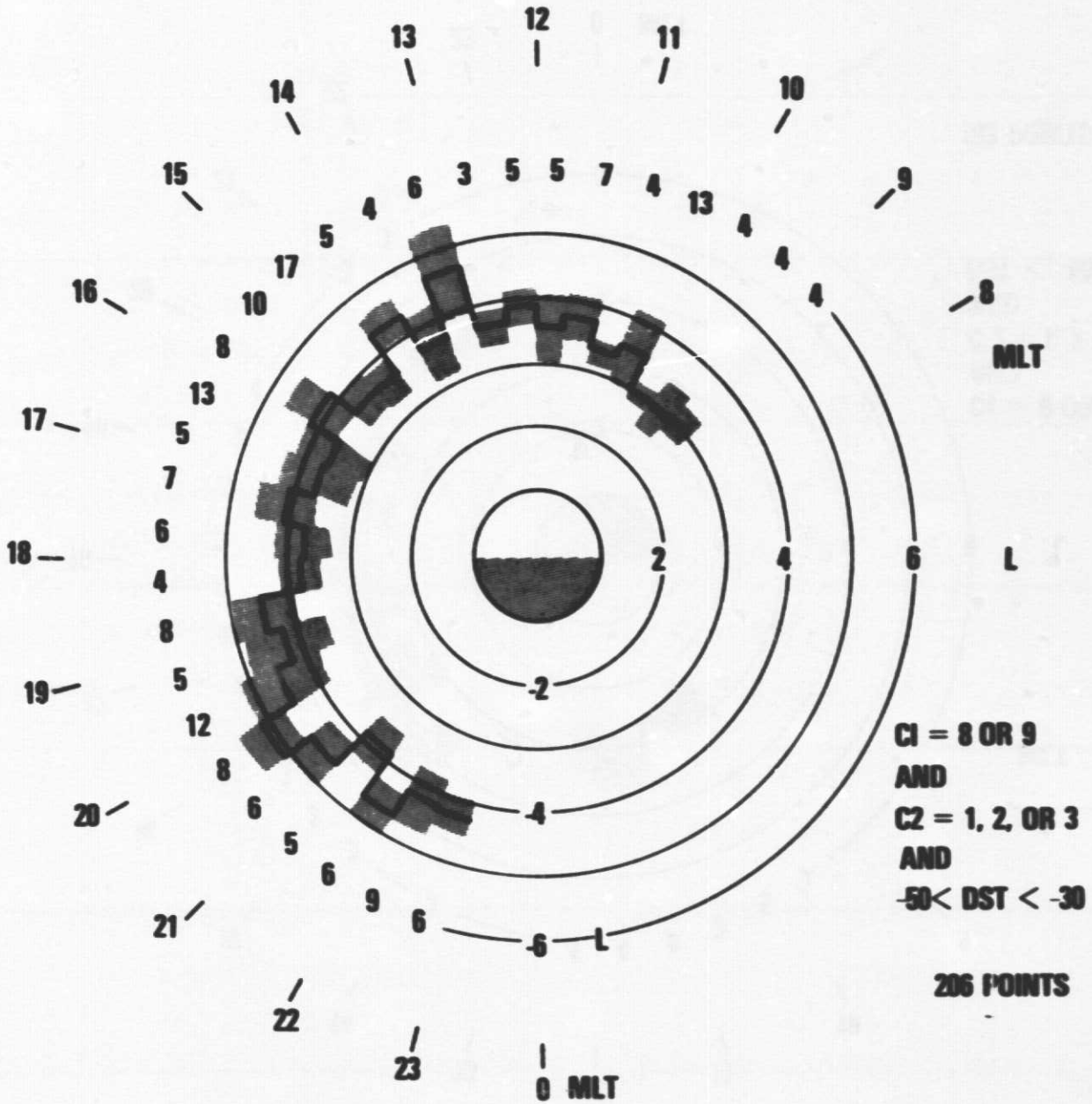
12
13
11
14
10
15
9
16
8
MLT
17
18
L
19
20
21
22
23
0 MLT
-2
-4
-6
2
4
6
C1 = 8 OR 9
AND
C2 = 1, 2, OR 3
AND
-50< DST < -30
206 POINTS

Figure 5c

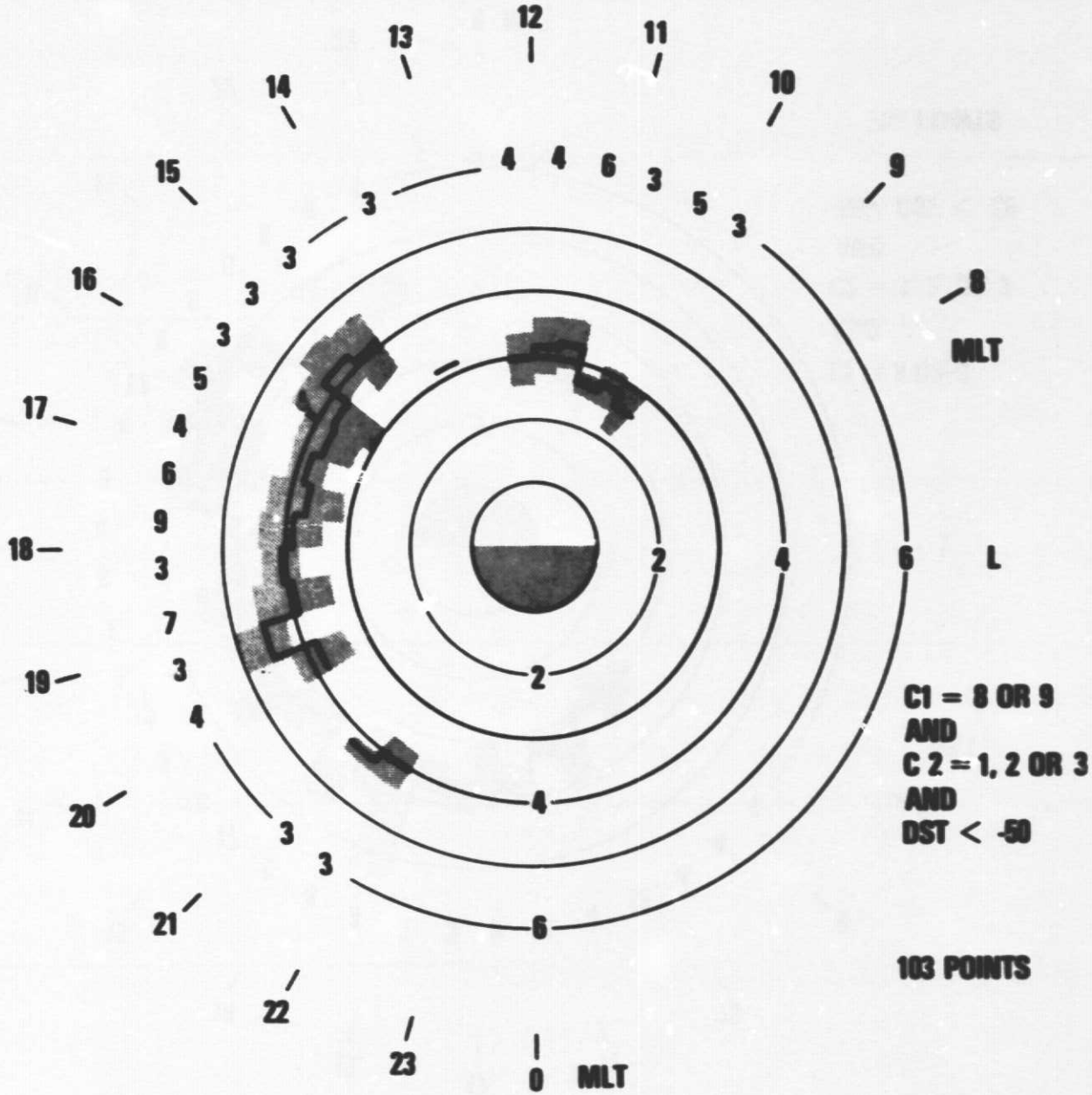
12
13
11
14
10
15
9
16
8
MLT
17
18
L
19
20
21
22
23
0 MLT
C1 = 8 OR 9
AND
C 2 = 1, 2 OR 3
AND
DST < -50
103 POINTS

Figure 5d

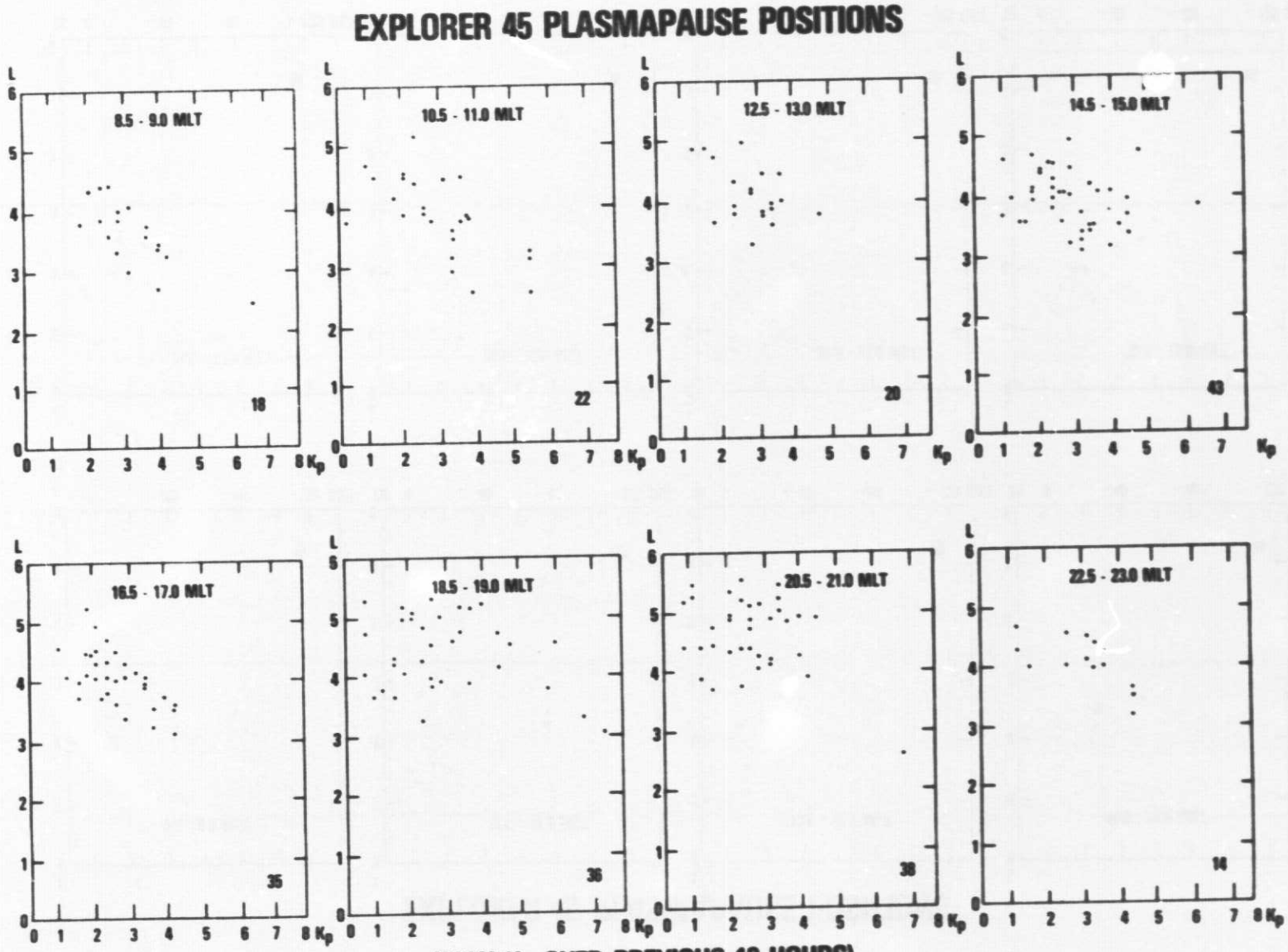
EXPLORER 45 PLASMAPAUSE POSITIONS
8.5 - 9.0 MLT
18
10.5 - 11.0 MLT
22
12.5 - 13.0 MLT
20
14.5 - 15.0 MLT
43
16.5 - 17.0 MLT
35
18.5 - 19.0 MLT
36
20.5 - 21.0 MLT
38
22.5 - 23.0 MLT
14
L
Kp
(MAX Kp OVER PREVIOUS 12 HOURS)

Figure 6

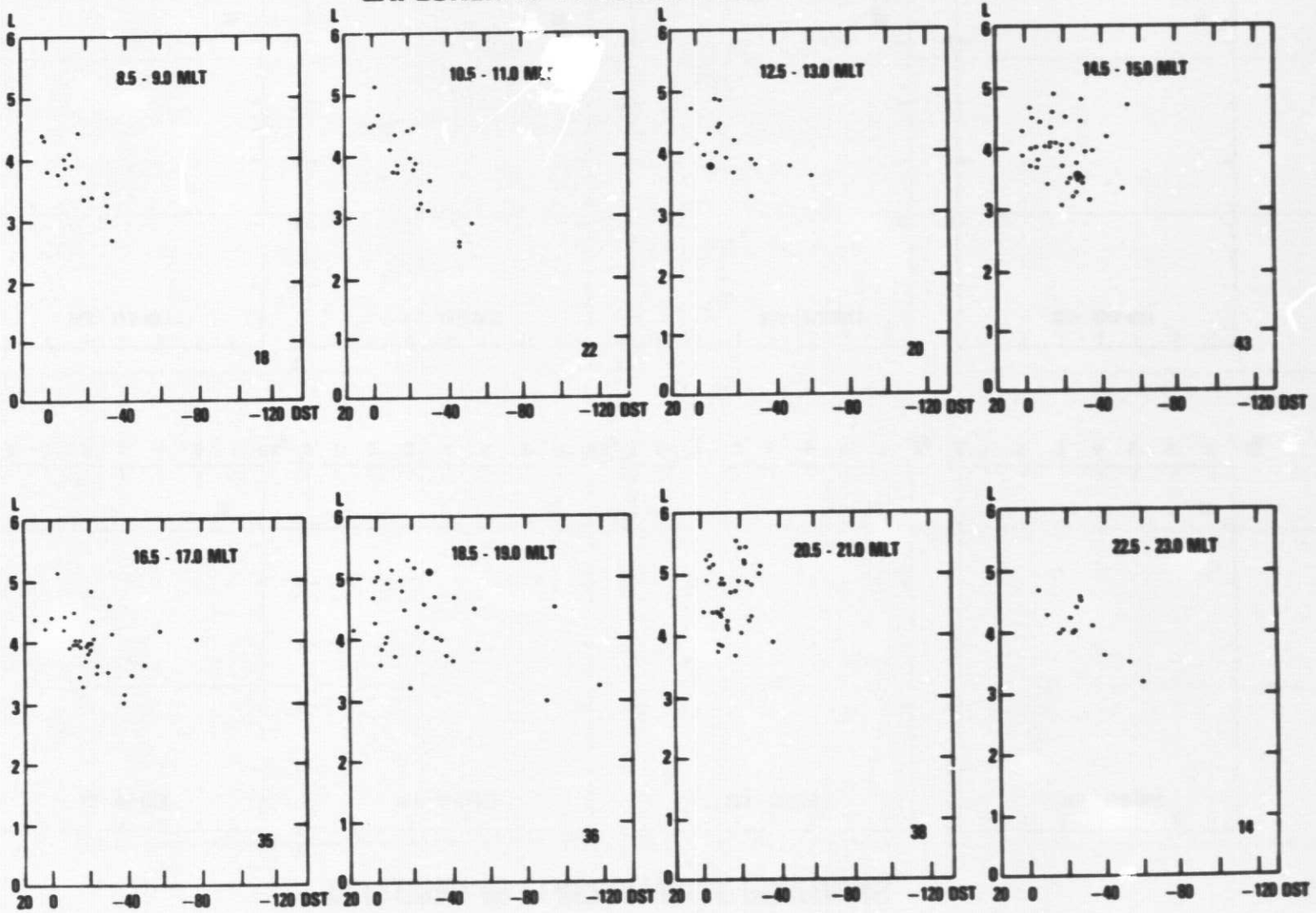
EXPLORER 45 PLASMAPAUSE POSITIONS
8.5 - 9.0 MLT
18
10.5 - 11.0 MLT
22
12.5 - 13.0 MLT
20
14.5 - 15.0 MLT
43
16.5 - 17.0 MLT
35
18.5 - 19.0 MLT
36
20.5 - 21.0 MLT
38
22.5 - 23.0 MLT
14
L
DST

Figure 7

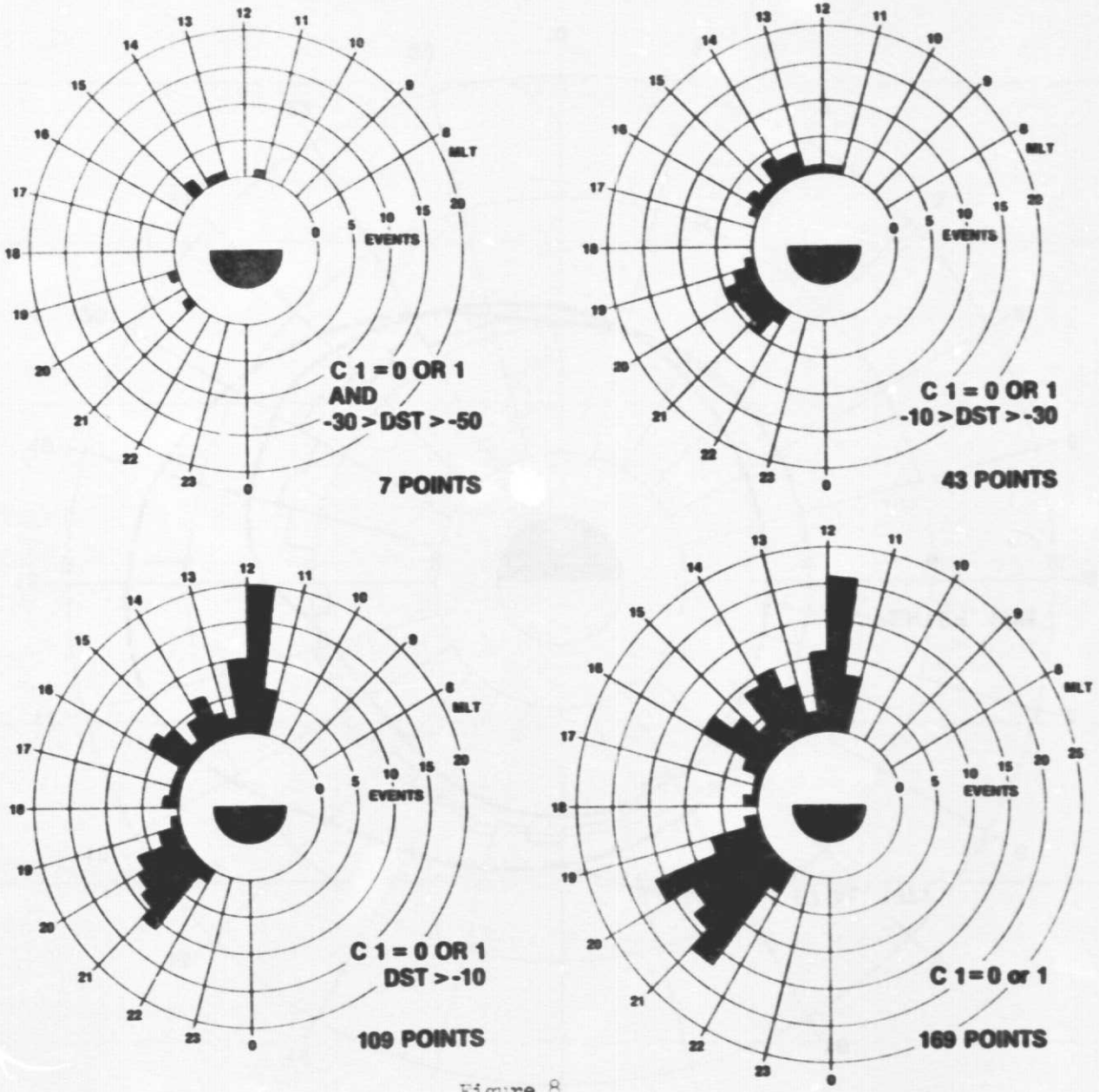
MLT
EVENTS
C 1 = 0 OR 1
AND
-30 > DST > -50
7 POINTS
C 1 = 0 OR 1
-10 > DST > -30
43 POINTS
C 1 = 0 OR 1
DST > -10
109 POINTS
C 1 = 0 or 1
169 POINTS

Figure 8

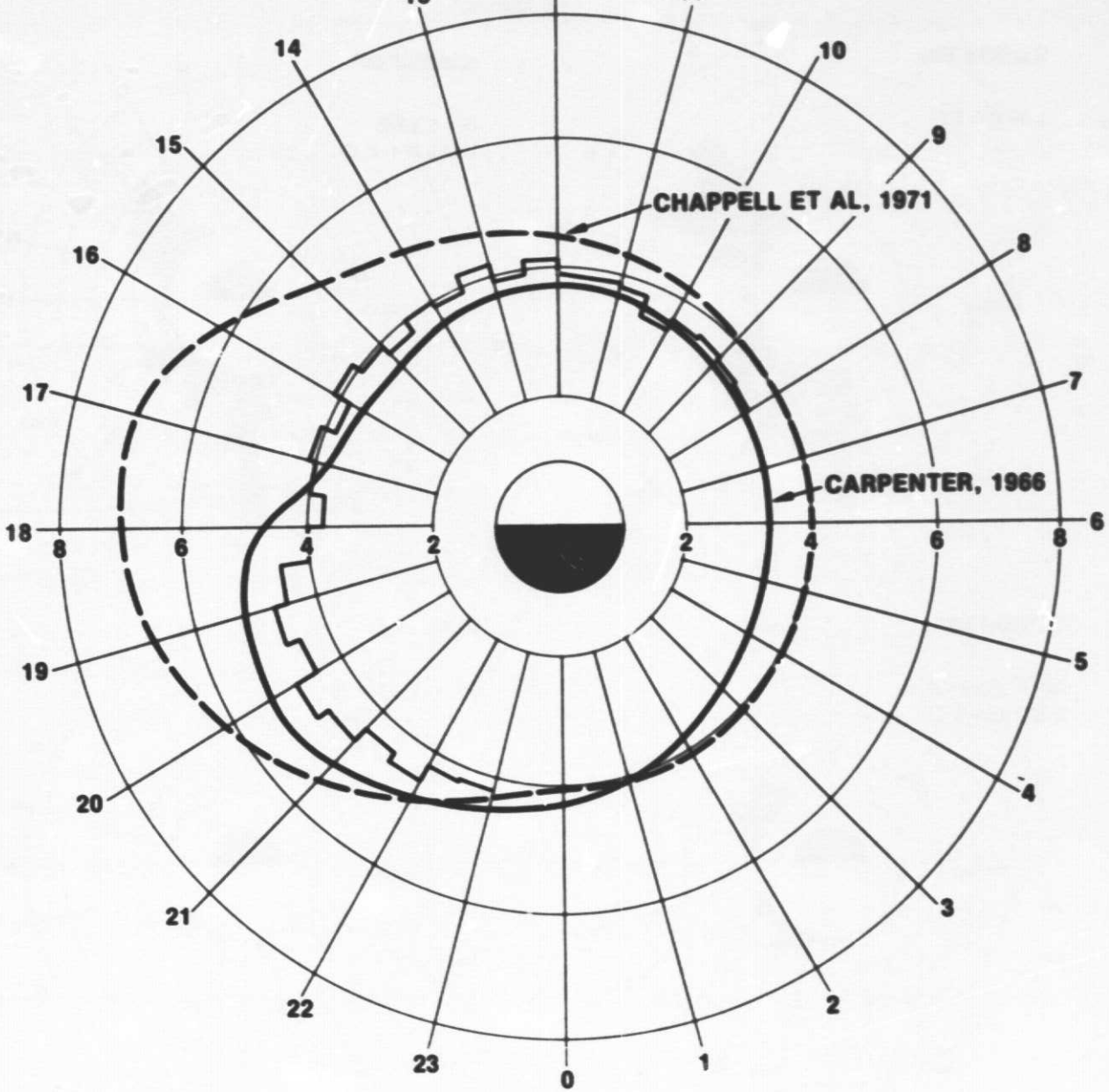
CHAPPELL ET AL, 1971
CARPENTER, 1966
14
10
15
9
16
8
17
7
18
6
19
5
20
4
21
3
22
2
23
1
0
8
6
4
2
2
4
6
8

Figure 9

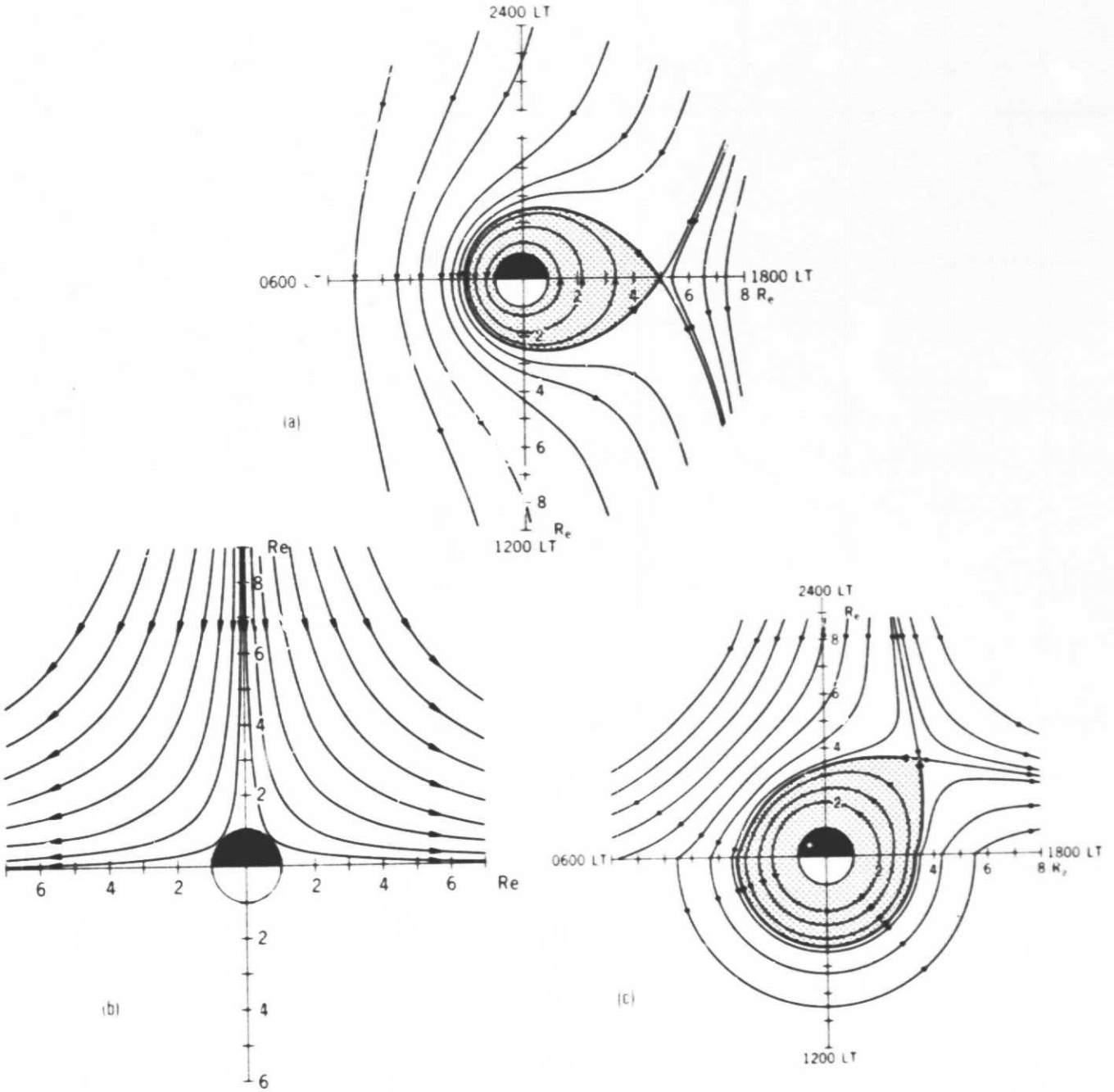

Figure 10